Materials Science and Engineering A329–331 (2002) 675–679

MATERIALS SCIENCE & ENGINEERING A

www.elsevier.com/locate/msea

Microstructural characterization of (Ni, Cu) Al intermetallic compounds rapidly solidified

S. Garcia-Galan [a,*], C. Gonzalez-Rivera [a], O. Alvarez-Fregoso [b], J.A. Juarez-Islas [b]

[a] *Departamento de Metalurgia, Facultad de Química, UNAM, Ciudad Universitaria, Mexico, DF 04510, Mexico*
[b] *Instituto de Investigaciones en Materiales-UNAM, Circuito Exterior S/N, Ciudad. Universitaria, Mexico, DF 04510, Mexico*

Abstract

In order to investigate the effect of Cu-macroalloying and rapid solidification processing on NiAl intermetallic compounds, six alloys were studied. Four alloy compositions were inside the β-NiAl field, one alloy composition was in the upper limit of the β-NiAl field and one was far from this β-NiAl field going to the (β-NiAl–Cu_3Al) field. Lattice constant showed a continuous increase as the copper content increased. TEM observations carried out in as-rapidly solidified ribbons showed the presence of elongated β-NiAl grains in alloys with Cu contents <20 at.%. In alloys with Cu content >20 at.%, the presence of second phase particles of Cu_3Al was detected. Microhardness Vickers values in the rapidly solidified ribbons were always lower as compared with the as-cast ingots. Room temperature ductility of a (Ni, Cu) Al alloy showed values of 190.1 MPa of 0.2% yield strength, 293.3 MPa of ultimate tensile strength and 2.37% of elongation. © 2002 Elsevier Science B.V. All rights reserved.

Keywords: Intermetallic compound; Macroalloying; Rapid solidification; Mechanical properties

1. Introduction

NiAl intermetallic compounds possesses low density, good oxidation resistance and metal-like properties, which makes them attractive materials for a wide range of applications [1,2]. In this compound, the strong bonds and low symmetry of the deformation behavior, on the basis of ordered structure, give rise to low temperature embrittlement and inadequate strength and creep resistance at elevated temperatures [3].

On the other hand, the ductility of some intermetallics has been enhanced by macroalloying with a third element and by microstructural control through processing [4].

Solidification processing of intermetallic compounds upon equilibrium phase diagrams appear to be quite limited. With conventional melt processing of intermetallic compounds one or more peritectic reactions and wide liquidus–solidus separation are encountered leading to large-scale composition segregation which is difficult to eliminate during post-solidification treatments. At the same time, the characteristics which make intermetallic compounds unattractive for conventional processing, qualify them as suitable candidates for rapid solidification processing.

Since intermetallic compounds posses a variety of properties which would otherwise be beneficial for high temperature structural applications, a major objective of rapid solidification processing effects have been to improve their ductility, by taking advantage of its resulting effects, which include: (i) a decrease in grain size; (ii) manipulation of long range order or antiphase domain; (iii) large volume fraction of dispersoids; (iv) increase in point and line defects; and (v) increase in solubility of intermetallic compounds.

The purpose of this work was to present results on the effect of rapid solidification processing and Cu-macroalloying in the NiAl intermetallic compound.

2. Experimental procedure

In order to study the effect of rapid solidification processing and macroalloying on the NiAl intermetallic compound, Cu additions were made to the β-NiAl, substituting Ni for Cu by adding fixed concentration ratios, $x_{Ni/Cu} = (1-y)/y$ in the $Ni_{1-y}Cu_yA1$ system.

* Corresponding author.
E-mail address: sergiogg@servidor.unam.mx (S. Garcia-Galan).

PII: S0921-5093(01)01606-9

Table 1
Chemical composition of rapidly solidified ribbons (in at.%)

Element	Alloy 1	Alloy 2	Alloy 3	Alloy 4	Alloy 5	Alloy 6
Al	49.9 ± 0.03	50.9 ± 0.04	48.0 ± 0.08	50.0 ± 0.05	49.5 ± 0.02	29.4 ± 0.09
Ni	45.4 ± 0.06	39.0 ± 0.06	36.7 ± 0.01	29.9 ± 0.07	25.9 ± 0.01	34.5 ± 0.04
Cu	4.6 ± 0.03	10.0 ± 0.01	15.2 ± 0.02	19.9 ± 0.08	24.5 ± 0.08	36.1 ± 0.06
Ni+Cu	50.0	49.0	$51.9 \pm$	49.8	50.4	70.6
$x_{Ni/Al}$	9.86	3.90	2.41	1.50	1.05	0.95
y	0.09	0.20	0.29	0.40	0.48	0.51

The (Ni, Cu) A1 intermetallic compound was prepared by using $x_{Ni/Cu}$ concentration ratios of 0.95, 1.05, 1.50, 2.41, 3.90 and 9.86. The high purity (99.99%) Al and electrolytic Ni and Cu (99.97%) elements previously weighted, were placed in a graphite crucible and melted under vacuum ($\sim 10^4$ mmHg). The induction furnace was switched off until an exothermic reaction was observed, and then the liquid melt was allowed to cool to room temperature.

During the melt spinning experiments, 50 g of the alloy was placed into a quartz crucible of 1.0-cm diameter and 10-cm length. The crucible was placed 1.0 cm from a copper wheel which was rotated at a speed of 15 m s^{-1}. Once the alloy was induction melted, argon gas was injected (6 psi) from the top of the crucible which spilled the liquid alloy into the rotating wheel, obtaining ribbons of 50-μm thickness and 3-mm width.

Microstructural characterization of the rapidly solidified ribbons was carried out by a Stereoscan 440 scanning electron microscope (SEM), a JEOL 2100 scanning transmission electron microscope (TEM) and a Siemens D-5000 X-ray difractometer. Microhardness Vickers measurements were carried out in a Matzusawa microhardness tester by employing a 15-g load. The tensile test on ribbons was performed on an Instron 1125 Machine.

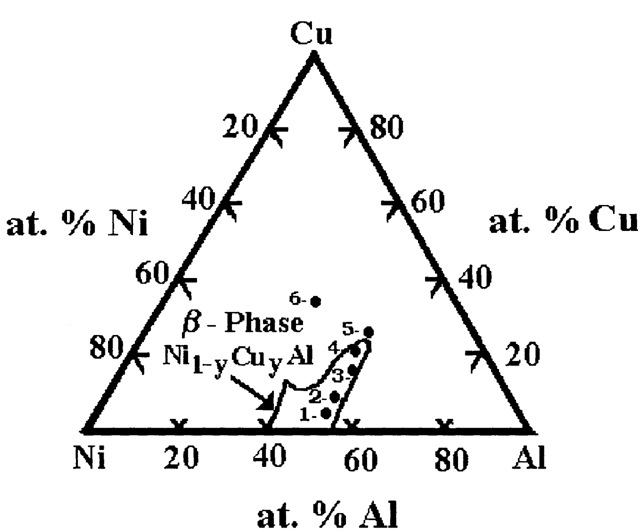

Fig. 1. Ternary Ni–Cu–Al phase diagram [5], where the location of the alloys under study is shown.

3. Results and discussion

The chemical composition of the alloys under study is shown in Table 1, together with the concentration ratio, $x_{Ni/Cu}$, and the y-value. Fig. 1 shows the ternary Ni–Cu–Al phase diagram as reported by Lipson and Taylor [5], where the ternary-field of the solid solubility of Cu in β-NiA1 at room temperature is shown. This solid solubility field extends far in the direction of Ni_{1-y} Cu_yA1 for a maximum of $y = 0.46$ [6]. In the same figure and indicated, the location of the six alloys of interest is shown. Here it can be observed that four alloy compositions were inside the β-NiAl field, one alloy composition lies in the upper limit of the β-NiAl field and one alloy composition was far from this β-NiAl field going to the (β-NiAl–Cu_3Al) field.

Regarding lattice constant, it can be mentioned that the lattice constant of the stoichiometric NiAl inter-

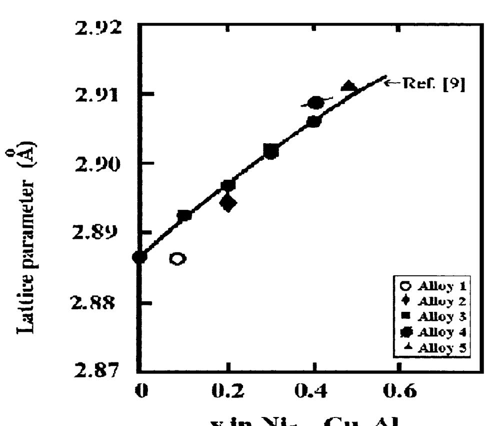

Fig. 2. Lattice parameter values determined in (Ni,Cu) Al alloys in the as rapidly solidified conditions as a function of y.

Table 2
Lattice parameter of (Ni, Cu)Al intermetallic compounds

Alloy	y	As-cast (Å)	As-rapidly solidified (Å)
1	0.09	2.889	2.888
2	0.20	2.898	2.893
3	0.29	2.902	2.901
4	0.40	2.907	2.907
5	0.48	2.908	2.911

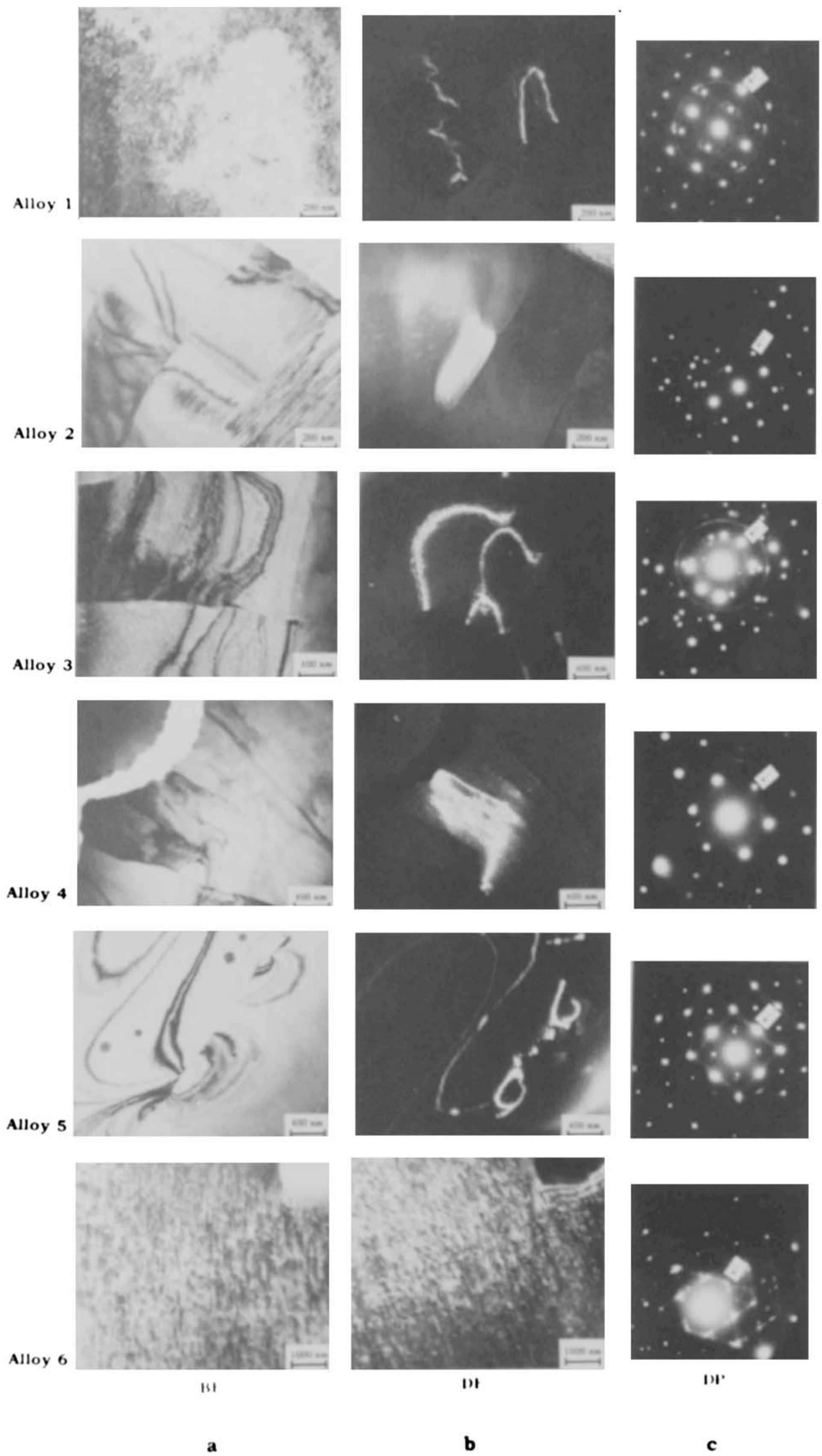

Fig. 3. TEM micrographs of the alloys under study: (a) bright field image, (b) dark field image and (c) diffraction pattern. Arrow in diffraction pattern shows the position where the dark field image was taken.

Table 3
Microhardness Vickers in as-cast ingots and in as-rapidly solidified ribbons

Alloy	Ingots (50 g load) (kg/mm^2)	Ribbons (25 g load) (kg/mm^2)
1	366 ± 32	320 ± 15
2	406 ± 24	370 ± 33
3	463 ± 35	430 ± 30
4	497 ± 18	465 ± 15
5	548 ± 20	517 ± 25
6	430 ± 18	492 ± 38

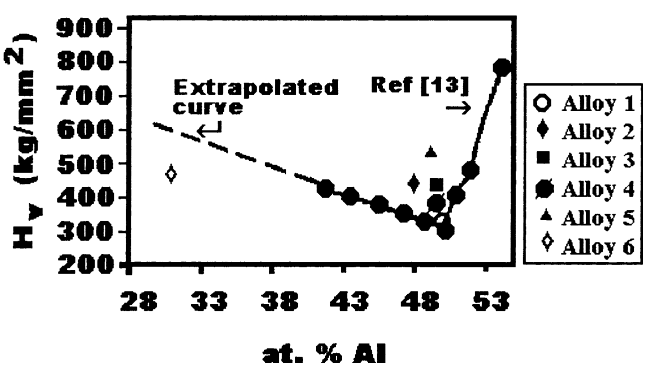

Fig. 4. Microhardness Vickers data for NiAl as a function of Al content [8], together with microhardness Vickers data for the alloys under study.

metallic compound at room temperature is 2.887 Å [7]. Table 2 presents the lattice parameter value determined in the (Ni, Cu) Al alloys in the as-cast and in the as-rapidly solidified conditions. As can be observed, when Cu substitutes Ni, the lattice parameter as a function of alloy concentration is shifted to higher values for both the as-cast ingots and rapid solidified ribbons, as is shown in Fig. 2. The same trend was reported by Jacobi and Engell [6] and this effect was explained as a result of the small difference in atomic radii of Cu and Ni.

TEM observations carried out in rapidly solidified ribbons, showed the presence of elongated β-NiAl grains of ~4500 nm in length and 1200 nm in width for alloys 1–5, as shown in Fig. 3a. Dark field images (Fig. 3b) were taken in the (110) plane, as indicated in the diffraction patterns (Fig. 3c).

In alloy 5, the presence of second phase particles in the β-NiA1 matrix with diameters of ~200 nm was observed. These second phase particles were identified by means of TEM microanalysis as Cu_3A1. Regarding alloy 6, the related microstructure is shown in Fig. 3, where the presence of the β-NiAl matrix with second phase particles can be seen.

Table 3 shows microhardness Vickers data for as-cast ingots and rapidly solidified ribbons, where it is found that microhardness values in the rapidly solidified condition showed a decrease as compared with microhardness values in the as-cast ingots.

Microhardness Vickers values for NiAl as a function of Al content has been reported by Westbrook [8] and is shown in Fig. 4 (full line). This figure shows that the ordered B2 NiAl compound exhibits a minimum at the stoichiometric composition. This behavior was explained [9] in terms of a minimum, at stoichiometric composition, of vacancies (Al-rich) and antisite defects (Ni-rich). The microhardness Vickers values of the alloys under study are also shown in this figure, for the rapidly solidified ribbons. Here it can be seen that alloys 1–5 showed microhardness values higher than those reported by Westbrook [8] and that alloy 6 showed microhardness below the extrapolated curve.

On the other hand, room temperature ductility of polycrystalline NiAl can range from 0 to 2.5% depending upon stoichiometry [10], texture [11], grain size [12] and possible impurity content and structure.

For the alloys under study, alloys 1–5 showed 0% ductility, and tensile tests performed on four ribbons of alloy 6 showed 190.1 ± 2.8 MPa of 0.2% of yield strength, 293.3 ± 8 MPa of ultimate tensile strength and $2.37 \pm 0.25\%$ of elongation. A representative plot of stress versus elongation for this alloy is shown in Fig. 5.

4. Conclusions

The effect of Cu-macroalloying and rapid solidification processing on NiAl intermetallic compounds showed an improvement in room temperature ductility, reaching values up to 2.36% of elongation, for continuous ribbons with Cu contents up to 36 at.%. This encouraging result suggests that further research must

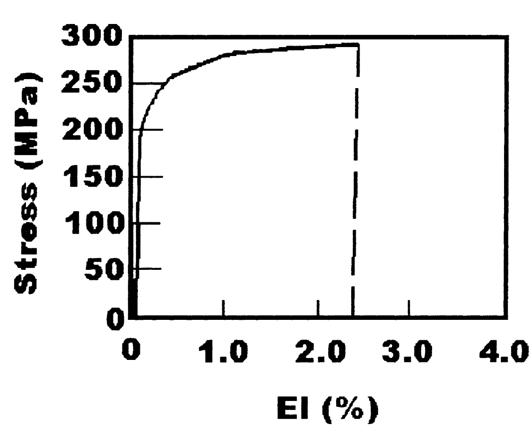

Fig. 5. A representative plot of stress versus elongation of rapidly solidified ribbons of alloy 6.

be carried out on the Ni-rich side of the stoichiometric NiAl, by substituting Ni for Cu and working in the β-NiAl field or in the β-NiA1/Cu_3AI field.

Acknowledgements

The authors acknowledge the contribution of Mr E. Caballero, Eng. L. Baños, A. Maciel and Tech. R. Guerrero, during the experimental work.

References

[1] D.B. Miracle, Acta Metall. 41 (1993) 649.
[2] R.D. Neobe, R.R. Bowman, M.V. Nathal, Int. Mater. Rev. 38 (1993) 193.
[3] D.B. Miracle, R. Darolia, in: J.H. Westbrook, R.L. Fleisher (Eds.), Intermetallic Compounds, vol. 2, John Wiley and Sons Ltd, 1994, p. 53.
[4] I. Backer, P.R. Munroe, J. Met. 40 (1986) 28.
[5] H. Lipson, A. Taylor, Proc. R. Soc. A173 (1939) 232.
[6] H. Jacobi, H.J. Engell, Acta Metall. 19 (1971) 701.
[7] A. Taylor, N.J. Doyle, J. Appl. Crystallogr. 5 (1972) 201.
[8] J.H. Westbrook, Metallurg. Rev. 9 (1964) 415.
[9] I. Baker, Mater. Sci. Eng. A 192 (1995) 1.
[10] K.H. Hahn, K. Vedula, Scr. Metall. 23 (1989) 7.
[11] K. Vedula, K.H. Hahn, B. Boulogne, in: C.T. Liu, A.I. Taub, N.S. Stoloff, C.C. Koch (Eds.), High Temperature Ordered Intermetallic Alloys III, MRS Proceedings 133, 1989, p. 299.
[12] E.M. Schulson, D.R. Baker, Scr. Metall. 17 (1983) 519.